ISSN 1330-3651 (Print), ISSN 1848-6339 (Online)
https://doi.org/10.17559/TV-20230523000660
Original scientific paper

Iron Intermetallic Compounds (IMCs) Formation Mechanism in the Molten Aluminium Zinc (Al-Zn) Coating Alloy

Abdul KHALIQ*, Vishnu KASVA, Abdulaziz S. ALGHAMDI, Mohamed RAMADAN, Tayyab SUBHANI, Waseem HAIDER, K. S. Abdel HALIM

Abstract: To prevent corrosion of steel products, the steel industry often relies on Al-Zn based alloy coatings, applied through hot-dip coating technology. Despite this, a long-standing problem in the galvanizing industry involves the formation of Fe-based intermetallic compounds (IMCs) in the Al-Zn coating bath, caused by iron dissolution from steel products. Such IMCs are the primary source of dross formation in the Al-Zn bath, which inevitably leads to metal spot defects in the coated steel products and bottom dross build-up in the Al-Zn bath. The present research aims to investigate the mechanism of Fe transformation into IMCs. To achieve this, Fe saturated and unsaturated Al-Zn alloys were doped with low carbon steel at a temperature of 600 °C. The samples were collected at regular intervals and quenched in water. The optical microscopy (OM) and scanning electron microscopy (SEM) with energy dispersive x-ray spectroscopy (EDS) were used to study the transformation of steel strips into Fe-IMCs particles in molten Al-Zn alloys. The study findings suggest that the Fe transformation into Fe-IMCs is a complex process, where the steel strip surface is initially oxidized, and Al_5Fe_2 and Al_3Fe are formed, which finally transform into Al_8Fe_2Si(Zn) (τ5c) IMCs particles. These results can assist galvanizers in understanding formation of Fe-IMCs and bottom dross build up in the costing pots.

Keywords: Al-Zn alloy; coating; dross formation; galvanizing; IMCs

1 LITERATURE REVIEW

Steel products are coated with zinc (Zn) and aluminium-zinc (Al-Zn) alloys for protection against corrosion and the process is called galvanizing. Steel products are dipped in the molten Al-Zn coating alloys that produce thin coating layer composed of Al-Zn matrix and iron intermetallic compounds (Fe-IMCs) [1]. Iron enters into the coating pot from steel products by following two routes. (1). Fe particles attached to the surface of the steel products, (2). Steel products dissolution during dipping that release Fe. This Fe transforms into Fe-IMCs regardless of their incoming route [2]. The presence of Fe in liquid Al-Zn bath transforms into the Fe-IMCs, which at later stages leads to the development of bottom dross in the coating pot. The Fe-IMCs layer between Al-Zn overlay and steel substrate improve corrosion resistance of steel products [3, 4]. One of the possible solutions to avoid development and growth of Fe-IMCs is to control the amount of Fe in liquid bath, which can be attained by managing the diffusion of Fe in Al-Zn bath, which ultimately reacts with Al and precipitates in the form of Fe-IMCs. Literature identified that by avoiding the saturation of Fe in liquid Al-Zn alloy, Fe-IMCs formation can be retarded and also reversed by their dissolution [2, 5, 6].

The Fe solubility in the 55 wt.% Al-Zn bath has been comprehensively investigated [2]. A heat of molten bath weighing 12 kg was kept in a pot at a temperature range of 568 ºC to 700 ºC. Approaching the maximum temperature, the Al-Zn melt was supersaturated with Fe and later kept untouched for several hours before sampling. Melt stirring was continuously performed to maintain uniform temperature in the molten bath, which allowed settling of the suspended Fe-IMCs particles at bottom of the pot. When the sampling process was started, the first sample was carefully taken from the top melt layer without causing any disturbance to the particles at the bottom melt layer. The sample size of 5 mm in diameter and 100 - 150 mm in length was taken. In order to acquire precise results, several samples were taken by repeating the sampling process. Any lowering of temperature of the Al-Zn melt during sampling process was immediately attained due to the presence of isothermal sensors [2]. The following equation determines the solubility of Fe with reference to temperature, as measured in kelvin (K):

$$\text{Fe (wt.\%)} = \exp\left[7.48 - (7203/T)\right] \quad (1)$$

Eq. (1) indicates that quantity of Fe is directly proportional coating the pot temperature [2]. A concise summary of the change in solubility of Fe with temperature has been reported by [2]. It shows that Fe dissolves in the bath at a temperature above 560 ºC. The accurate results of the exact solubility of Fe in bath are absent. However, the industrial liquid melt has 0.4% Fe at a temperature of 600 ºC [2, 7]. It is to be noted that the suspended dross particles are always present in the liquid bath and it is impossible to avoid these particles during sampling at the Fe solubility below 0.40%. Upon coming in direct contact with the molten Al-Zn alloy, the Fe atoms releases from the steel substrate and dissolve in the melt [10]. Thermodynamic calculations indicate that the transient Fe solubility is greater than that of the equilibrium Fe solubility. It is assumed that the reaction of Fe and Al forms complex Fe-IMCs which obviously decrease the solubility of Fe in the melt. Furthermore, rise in the Al content in the Galvalume melt increases the dissolution of Fe in the solution [11].

The sampling of Fe-IMCs in different conditions has been investigated by other studies [10]. In a study [2], it was noted that the splat quenching of samples from the pot is more effective than slow conventional cooling down to room temperature and is helpful in preserving the actual bath conditions. It is further believed that during conventional cooling, the precipitations and growth of the Fe-IMCs such as AlFeSi is unavoidable. Moreover, α-AlFeSi and β-AlFeSi phases were detected in the SEM/EDS [12, 13]. In addition to that Fe-IMCs particles

τ5C with composition of 56wt% Al-32.6wt%Fe-6.1wt%Si-5.3wt%Zn were also observed.

The splat-quenched sampling technique offers advantage of easily identifying the suspended dross Fe-IMCs. The small particles have a size range of 2-5μm while larger particles are > 20 - 100 μm. These Fe-IMCs particles grow due to their clustering. Al-oxides thin phases floating on top surface of the Al-Zn alloy have also been reported in literature [14, 15].

The microstructures of hard and mushy bottom Fe-IMCs were observed by optical and scanning electron microscopy and reported by the previous researcher [2]. Mushy dross was studied both before and after the Zn enrichment. It was found that hard bottom dross was rich in Zn content. It has been reported that Zn enrichment has altered the mushy dross, and as a result, no cohesive network was found in the IMC particles [16, 17]. Hence, it can be inferred that the Zn enrichment helps in breaking the cohesive network of fine particles of the hard bottom dross.

The dross Al_8Fe_2Si (Zn), Fe-IMCs particles are recognised as τ5c and are main source of metal spot defects in the coated steel strip and flat products. Fine mushy dross particles of size up to 5 μm are entrapped in the overlay region of the Al-Zn coating [18, 19]. Once flat steel strips passed through the final rolling step, τ5c Fe-IMCs experience compressive forces. The Fe-IMCs are hard and brittle hence fractured and produced ents in the relatively ductile steel strips and overlay coating [20]. Such defects are called the metal spot defects which ultimately compromise the corrosion resistance and overall quality of coated steel products. Dross particles grow by coarsening and agglomeration in the coating pot. Coarsening mechanism is dominant during bath temperature fluctuation. However, agglomeration growth is a continuous phenomenon and is accelerated by molten Al-Zn alloy stirring. Once dross particles grow beyond > 10 - 100 μm, their settling in the bottom of the pot becomes dominant and leads to the bottom dross build-up. Removal of the bottom dross becomes unavoidable after its height increased to a certain critical level in the Al-Zn coating pot. For this, continuous hot-dip coating lines are stopped and massive operation is needed to remove the hard bottom dross [5].

An extensive literature investigation revealed that the galvanizing pot conditions are dynamic hence Fe saturated and unsaturated regions are inevitable. Therefore, Fe-IMCs formation and the bottom dross build-up in the coating pot remained a long standing issue in the galvanizing industry. An explicit mechanism of Fe particles transformation into Fe-IMCs is absent in the literature.

The aim of this study is to elucidate Fe conversion into Fe-IMCs in Al-Zn coating alloy under industrial temperature conditions of 600 °C. For this Fe immersion and Fe-IMCs formation in Fe-saturated (actual bath conditions) and Fe-unsaturated molten Al-Zn alloy have been studied. This study shall explain Fe particles transformation into Fe-IMCs. Fe- particles come with steel products during the hot-dip galvanizing process and transform into IMCs. Finally, Fe conversion mechanism into the bottom dross Fe-IMCs (τ5c) will be proposed based on the findings of this work. This study shall be helpful to understand the bottom dross build-up in the galvanizing pot. As a result, bottom dross management strategies can be formulated to improve quality of the coated steel products and also efficiency of the galvanizing process.

2 EXPERIMENTAL PLAN AND METHODOLOGY

For this study, weighed ingots of Al-Zn-Si alloy were melted in a clay-bonded graphite crucible using a resistance heating furnace. The alloy temperature was maintained at 600 ± 5 °C using a K-type thermocouple. Weighed amount of low carbon steel strip (ASTM A36) was immersed in the molten alloy using a stainless steel wire. The steel strip was added as a source of iron (Fe) to achieve required Fe level in the Al-Zn alloy. The Al-Zn-Si alloy and low carbon steel compositions are given in Tab. 1. The experimental set-up adopted was similar to that reported earlier [21]. The difference is that low carbon steel strip is immersed in the Al-Zn melt instead of the 316L stainless.

Table 1 Al-Zn alloy and low carbon steel composition

Elements	Al	Zn	Si	Fe	Mn	Minor
Al-Zn alloy - Fe saturated	55	43	1.6	0.4	-	Bal.
Al-Zn alloy - Fe unsaturated	55	43	1.6	0.2	-	Bal.
Steel strip	-	-	-	99	0.75	Bal.

The experimental plan consists of melting two batches of Al-Zn alloy. During 1st batch, 1100 g of Fe-saturated (0.40%) Al-Zn alloy was melted at 600 °C followed by 10 g carbon steel strip immersion. The aim is to investigate Fe conversion into IMCs particles at 600 °C when Al-Zn bath is already Fe-saturated. However, 2nd batch was composed of 1100 g of Fe-unsaturated (Fe: 0.20%) alloy where 6 g carbon steel was immersed. The rational of using Fe-unsaturated Al-Zn alloy was to investigate Fe conversion into IMCs particles when Al-Zn alloy is deficient with Fe. The industrial coating pot temperature fluctuations results in the Fe-IMCs precipitations. However, with temperature increase, Fe-unsaturated melt regions are expected in the coating pot.

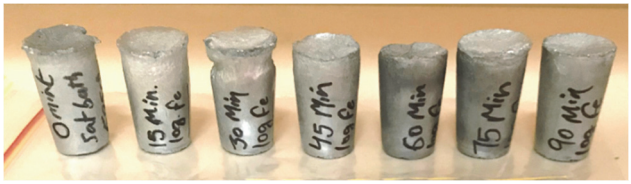

Figure 1 Batch No. 1 Samples - Iron saturated Al-Zn melt (starting bath 0.40% Fe and then Fe concentration raised to 0.66%)

The alloy samples were taken at regular time intervals of 0, 15, 30, 45, 60, 75 and 90 minutes and quenched in water to avoid IMCs growth during solidification process. Both batches samples taken at regular time intervals are shown in Fig. 1 and Fig. 2 that are cylindrical and weigh 10 - 15 g. Samples were sectioned and mounted for further study. Samples grinding was carried out using 400, 600, 800 and 1200 SiC emery papers and water as a lubricant while applying a force of 20 N at 250 rpm. Polishing was performed using 6 μm and 3 μm diamond paste at rotation of 150 rpm and load of 15 N. Final polishing step involves application of alumina suspension at a load of 10 N and 150 rpm rotation for 10 minutes. During each step,

ultrasonic cleaning of the samples was performed to make sure grinded particles are flushed and removed completely.

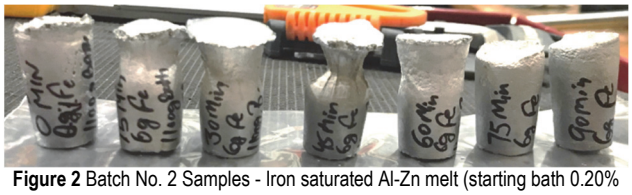

Figure 2 Batch No. 2 Samples - Iron saturated Al-Zn melt (starting bath 0.20% Fe and then Fe concentration raised to 0.40%)

3 CHARACTERISATION TECHNIQUES

The scanning electron microscope (SEM) model Philips XL 30 and an optical microscopy (Leica DM 2500) were used to investigate Fe conversion into IMCs particles in the Al-Zn alloy. Low carbon steel strip dissolution in Al-Zn alloy and Fe-IMCs formation mechanism were investigated with the support of microstructural features of the quenched samples. The SEM was equipped with energy dispersive x-ray spectroscopy that shall facilitate to identify various types of Fe-IMCs in the Al-Zn alloy.

4 RESULTS AND DISCUSSION

4.1 Optical Microscopy (OM) Analysis

Fig. 3 shows optical microscope image of the batch 01 samples taken after 15, 30, 75 and 90 minutes of low carbon steel immersion in the Al-Zn melt at 600 ºC. In this batch Fe-saturated Al-Zn alloy was melted and 10g of steel strip was added to raise Fe concentrations to 0.66%. It is aimed that Fe from steel strip will convert into Fe-IMCs directly considering Al-Zn bath is already Fe-saturated. The Fe-IMCs formation is evident from Fig. 3. IMCs shape and morphologies are distinct hence can be argued that these IMCs are unique. They are formed at various stages during Fe interaction with the Al-Zn bath.

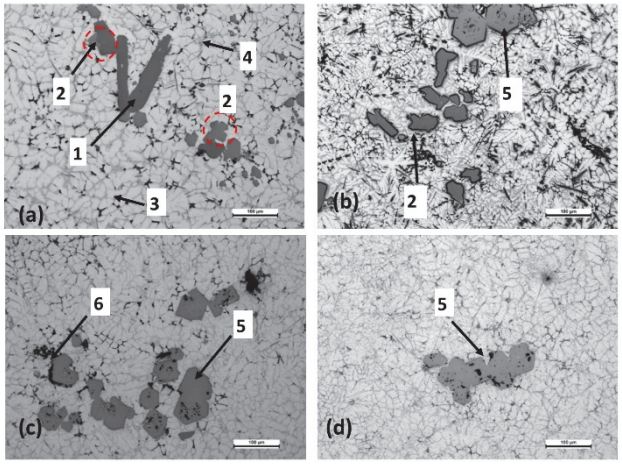

Figure 3 Optical microscopy images of Batch 01 (a). 15 mint, (b). 30 min, (c). 60 min and (d). 90 min

It is clear from Fig. 3a that steel has been fragmented once immersed in the Fe-saturated Al-Zn bath. There is no evidence of gradual dissolution of the strip. There is a direct solid-liquid reaction that resulted in the formation of 1st stage of Fe-IMCs. At this stage, crystallography of the Fe- IMCs is not clear. This Fe transformation is marked as 1 in Fig. 3a. Once Fe has converted into 1st type of IMCs in the Al-Zn bath, 2nd types of IMC are nucleated from the 1st type surface, as can be seen from Fig. 3a marked as 2. Finally, 2nd type of Fe-IMC particles is converted into 3rd type of IMC particles that are hexagonal in shape and also exhibit distinct morphology, marked as 5 in Fig. 3b, Fig. 3c and Fig. 3d. These IMCs particles are most likely τ5c and are responsible for bottom dross formation in the Al-Zn coating pot. These τ5c IMC particles are main source of metal spot defects in the overlay of the coated steel strip products. It has been established that the Fe particles once entered the Fe-saturated Al-Zn bath convert into τ5c IMC particles gradually.

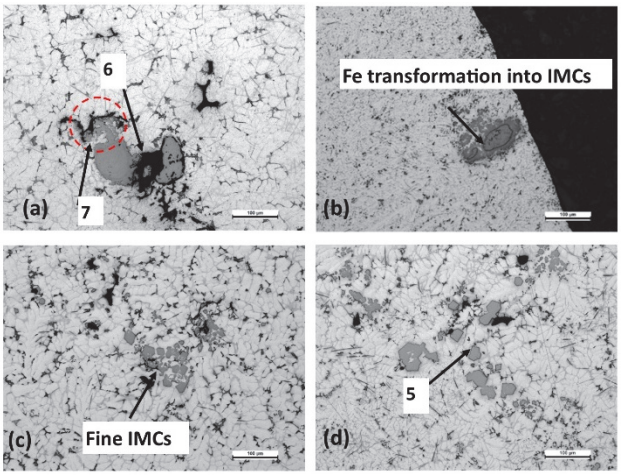

Figure 4 Optical microscopy images of Batch 02 (a). 15 mint, (b). 30 min, (c). 60 min and (d). 90 min

The base microstructure of the Al-Zn coating alloy is similar to that reported by the previous researchers [12] which is composed of α-Al matrix (mark 3) and β-Zn (mark 4) in the inter-dendritic regions. IMC particles of Mg_2Si in the inter-dendritic regions of α-Al have also been reported in literature [12]. However, during optical microscopy analysis, it is challenging to distinguish Mg_2Si particles.

An optical microscopy image of the batch 02 samples is shown in Fig. 4. Fe-unsaturated Al-Zn alloy was melted and 6 g of low carbon steel strip was added to raise overall Fe contents to 0.40%. It was aimed to study Fe conversion into Fe-IMCs in case the Al-Zn bath is Fe-unsaturated at 600 ºC. Microstructural features are distinct and different to those of the batch 01 as can be observed from Fig. 4a and Fig. 4b. It is clear from Fig. 4a that steel strip is dissolving in the Fe-unsaturated Al-Zn bath. There is a strong driving force between highly Fe rich steel strip and Fe unsaturated Al-Zn bath that will facilitate steel strip dissolution and release of Fe into the Al-Zn bath. It is hypothesised that steel strip dissolution will be the 1st event in batch 02. Fe-IMCs of types 1, 2 and 3 will also form in to the Al-Zn bath similar to the batch 01. It should be noted that Fe solubility of 0.40% in the Al-Zn bath at 600 ºC is with reference to type 3 Fe-IMCs. In case Fe solubility of 0.40% is with reference to Fe in solution with the Al-Zn bath, Fe-IMCs should not precipitate during batch 02. Black regions shown in Fig. 3 and Fig. 4b represent steel strip oxidation during immersion stage that was unavoidable in the given experimental conditions. Another key observation is the Fe-IMCs was the particle size distribution during the batch 02 that is much finer compared to the batch 01.

4.2 SEM Analysis

The batch 01 samples SEM images taken after 15 min and 90 min of steel strip immersion in the Al-Zn bath are given in Fig. 5. Grey α-Al matrix with inter-dendritic β-Zn are base features of the microstructure. Fe fragments converted into type 1 Fe-IMCs are shown in Fig. 5a that are most likely Al_5Fe_2; however further investigation is needed. Red circle is indicating Al_5Fe_2 transformation into type 2 Fe- IMCs that is most likely Al_3Fe. Finally, type 3 Fe-IMCs are shown in Fig. 5b that have distinct morphology of hexagonal shape and are also agglomerated. These Fe-IMCs shape is similar to the particles found in the bottom dross of Al-Zn coating pots [5]. It has been reported in literature that these particles are Al_8Fe_2Si (Zn) and are represented as τ5c. Such individual Fe-IMCs have grown to > 100 μm in diameter. However, during agglomeration, their size increased many folds.

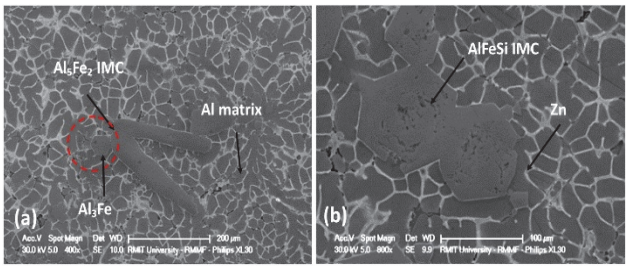

Figure 5 SEM images of samples taken after 15 min and 90 min of steel strip immersion into the Fe saturated Al-Zn bath at 600°C

4.3 Fe-IMCs Compositional Analysis and Their Identification

The Fe-IMCs compositional analysis was determined with energy dispersive x-ray spectroscopy (EDS). The EDS analysis of the batch 01 sample taken after 15 min of steel strip immersion in the Fe-saturated Al-Zn alloy bath is shown in Fig. 6. SEM image of Fe-IMCs and selected points for EDS analysis are shown in Fig. 6a. The long irregular phase shown in Fig. 6a is composed of 54% Al, 37.3% Fe, 1.4% Si and 1.9%Zn. Fig. 6b shows EDS analysis of point 42. Such Fe-IMCs phases are recognised as Al_3Fe (type 2) as has been reported by Chen and Yuen [12]. This suggests that Fe-fragments transformed to Al_3Fe within a short period of reaction (15 min). It is argued that solid Fe reaction with Al-Zn bath exhibits multistage core reaction. It is hypothesized 1st type of the Fe-IMCs (Al_5Fe_2) formed immediately when Fe particles interact with Fe-saturated Al-Zn bath. This argument can be supported with the fact that Al_5Fe_2 thin layer formed immediately when steel strip is dipped in the Al-Zn bath during continuous galvanizing process [16]. Considering longer reaction time (> 15 min) in this study, initially formed Fe-IMCs (Al_5Fe_2) are not observed during SEM analysis.

The EDS analysis of the hexagonal regular shaped phases is shown in Fig. 6c and Fig. 6d. These Fe-IMCs are composed of 57.9% Al, 29.4% Fe, 5.3% Si and 7.2% Zn, as shown by points 44 and 45 in Fig. 6a. This is a typical chemical composition of the Fe-IMCs particles found in the bottom dross of the Al-Zn coating pot. Khaliq et al. [10] reported similar chemical compositions of these Fe-IMCs particles. Therefore, it is suggested that these Fe-IMCs particles are τ5c which will remain unchanged with further interaction with the Al-Zn coating bath at 600 °C. Chemical compositions of batch 01 and batch 02 samples obtained by EDS are summarized in Tab. 2.

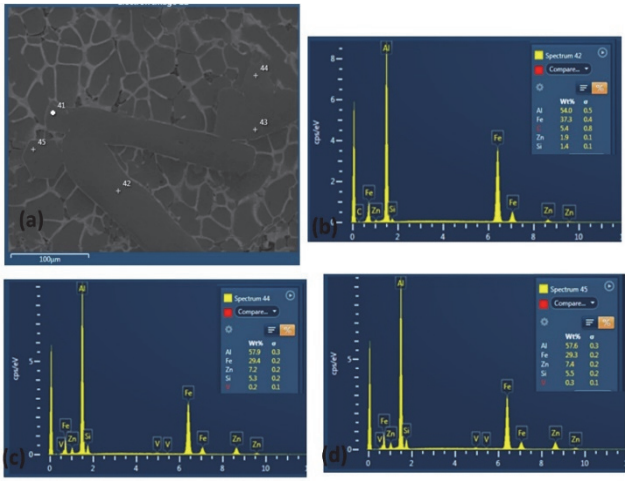

Figure 6 Fe-IMCs compositional analysis obtained by EDS when steel strip was immersed in the Fe-saturated Al-Zn bath at 600°C (a). SEM image, (b), 1st type Fe-IMCs, (b). 2nd type Fe-IMCs, (d). 3rd type Fe-IMCs

Table 2 Chemical composition of the Fe-IMCs phases in the Al-Zn coating alloy

EDS points	Al	Fe	Si	Zn	Cr	V	Phase identified
Batch 01 - 42 [this study]	54.0	37.3	1.4	1.9	-	-	Al_3Fe
Batch 01 - 44 [this study]	57.9	29.4	5.3	7.2	-	-	Al_8Fe_2Si(Zn), τ5c
Batch 01 - 45 [this study]	57.6	29.3	5.5	7.4	-	-	Al_8Fe_2Si(Zn), τ5c
Batch 02 - 31 [this study]	55.8	25.5	5.1	9.1	-	-	Al_8Fe_2Si(Zn), τ5c
Batch 02 - 37 [this study]	57.5	28.0	6.0	7.8	-	-	Al_8Fe_2Si(Zn), τ5c
Khaliq et al. [10]	56.1	27.7	6.9	8.1	0.4	0.5	Al_8Fe_2Si(Zn), τ5c
Garcia et al. [22]	57.8	27.9	6.3	7.3	-	-	Al_8Fe_2Si(Zn), τ5c
Selverian et al. [2]	57	30	6	7	-	-	Al_8Fe_2Si(Zn), τ5c
Khaliq et al. [10]	56.8	37.7	3.1	1.1	1.1	0.6	Al_3Fe

Elemental mapping of the batch 01 samples taken after 15 min of carbon steel strip immersion in the Fe-saturated Al-Zn alloy at 600 °C is shown in Fig. 7. The Al-Zn alloy matrix is composed of α-Al as is evident from Fig. 7b. Zinc segregate in the inter-dendritic regions of Al during solidification, is shown in Fig. 7c. The irregular and hexagonal phases in Fig. 7d are Al_3Fe and Al_8Fe_2Si (Zn), τ5c Fe-IMCs. Si and Mg are found in the same Al inter-dendritic regions and are most likely Mg_2Si IMCs that are given in Fig. 7e and Fig. 7f. Elemental mapping analysis confirms various elements and Fe-IMCs locations in the Al-Zn alloy.

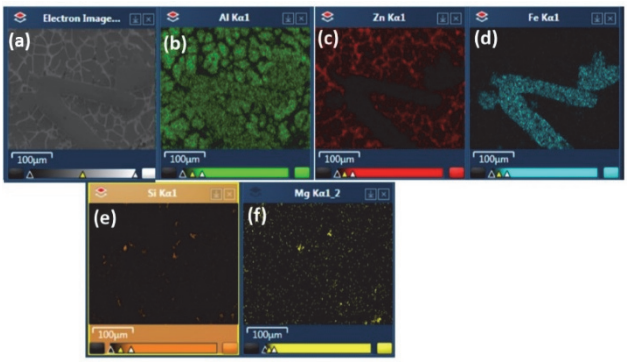

Figure 7 Elemental mapping of batch 01 samples taken after 15 minutes of steel immersion in the AL-ZN alloy at 600 °C

5 FE-IMCS FORMATION MECHANISM

Iron IMCs formation mechanism is proposed based on outcomes of this study and previous literature. In case the Al-Zn alloy bath is Fe-saturated, Fe particles entering the bath during steel strip immersion will convert into Al_5Fe_2 by solid-liquid reaction as given in Eq. (2). It is believed that this reaction is extremely fast and the resultant Fe-IMC (Al_5Fe_2) is unstable in the Al-Zn bath at 600 °C. Therefore, 1st type of Fe-IMCs (Al_5Fe_2) shall transform into 2nd type of relatively stable Fe-IMC phase.

$$5Al(l) + 2Fe(s) = Al_5Fe_2(s) \quad (2)$$

The Al_5Fe_2 transformation into Al_3Fe has also been reported by the previous investigators [11]. This is also a solid-liquid reaction that can be written as Eq. (3). Fe shall diffuse outwards from the unreacted Fe core. As a result, Al_5Fe_2 layer shall be maintained between Fe substrate and Al_3Fe IMC until core Fe is completely transformed into IMCs.

$$Al_5Fe_2(s) + Al(l) = 2Al_3Fe(s) \quad (3)$$

Finally, Al_3Fe IMC particles will transform into stable Al_8Fe_2Si IMCs particles that are recognised as τ5H. These IMCs particles possess hexagonal crystal structure. However, hexagonal crystal structure is converted into stable cubic structure by Zn doping in the Al-Zn coating bath. Therefore, Al_8Fe_2Si (Zn) Fe-IMCs are represented by τ5c that remain stable in the Al-Zn coating bath at 600 °C. The chemical reaction of Al_3Fe transformation into Al_8Fe_2Si (Zn) can be written as eEq. (4).

$$Al_3Fe(s) + Al(l) + Si(l) + Zn(l) = Al_8Fe_2Si\ (Zn)(s) \quad (4)$$

When Fe particles are immersed in the Fe-unsaturated Al-Zn bath (batch 02), ideally Fe particles should dissolve to raise Fe contents to the solubility limit of 0.40% at 600°C. If this Fe solubility limit of 0.40% is with reference to Fe in solution with the Al-Zn alloy, Fe-IMCs should not precipitate. However, Fe-IMCs are observed in the Fe-unsaturated Al-Zn alloy samples taken at regular time intervals as shown in Fig. 4. This shows that the Fe solubility of 0.40% in the Al-Zn alloy at 600 °C is with reference to Fe-IMCs (τ5c). In addition to that Fe-IMCs particles size in the Fe-unsaturated was finer compared to Fe saturated Al-Zn bath. The Al_8Fe_2Si (Zn), τ5c grow by coarsening and agglomeration in the Fe-saturated Al-Zn molten bath. Once τ5c particle size exceed threshold limit, it settled at the bottom of the coating pot as a bottom dross. Smaller τ5c particles leave the coating pot and become part of the overlay and finally become a source of metal spot defects.

6 CONCLUSION

This study investigated the formation of Fe-based intermetallic compounds (IMCs) in Fe-saturated and Fe-unsaturated Al-Zn molten alloy at 600 °C. The Al_8Fe_2Si (Zn) IMCs (τ5c) are the primary cause of bottom dross formation in the Al-Zn coating pot and metal spot defects in the rolled steel products, which has been a persistent problem in the galvanizing industry.

Iron particles will transform into Al_5Fe_2 by a solid-liquid reaction once immersed in the Fe-saturated Al-Zn bath. These Fe-IMCs are unstable hence shall transform into relatively stable Al_3Fe phase.

Stable Al_8Fe_2Si (Zn), τ5c Fe-IMCs are formed by the transformation of Al_3Fe at 600 °C. These Fe-IMCs are the main source of bottom dross build-up in coating pot and metal spot defects.

Fe transformation into stable τ5c IMCs is a complex and sequential process.

Agglomeration of τ5c Fe-IMCs has also been observed, with an increase in particle size over time leading to settling at bottom of the coating pot and formation of bottom dross. Removal of bottom dross requires shutdown of the continuous galvanizing coating lines.

Fe-IMCs presence in the Fe-unsaturated Al-Zn bath suggested that Fe solubility of 0.40% reported earlier [2] is with reference to τ5c IMCs rather than Fe in solution at 600 °C.

When steel strip was immersed, the size of Fe-IMCs particles was smaller in the Fe-unsaturated Al-Zn bath as compared to the Fe-saturated Al-Zn bath.

Acknowledgement

This research has been funded by the Scientific Research Deanship at the University of Ha'il-Saudi Arabia through project number RG-21 092.

The Microscopy and Microanalysis Facility (RMMF) of the RMIT University, Melbourne, Australia is acknowledged for the support and characterisation of the Al-Zn samples.

7 REFERENCES

[1] Marder, A. R. (2000). The Metallurgy of Zinc-Coated Steel. *Progress in Materials Science*, *45*, 191-271. https://doi.org/10.1016/S0079-6425(98)00006-1

[2] Setargew, N., Willis, D. J., & Thompson, D. (2004). Detection of Dross Intermetallic Particles in 55%Al-Zn Melt Using LAIS; *InterZAC*: Seoul, Korea, 1-16.

[3] Selverian, J. H, Notis, M. R, & Marder, A. R. (1987). The microstructure of 55 w/o Al-Zn-Si (Galvalume) hot dip coatings. *Journal of Materials Engineering*, *9*(2), 133-140. https://doi.org/10.1007/BF02833702

[4] Peng, W., Wu, G., Lu, R., Lian, Q., & Zhang, J. (2019). The evaluation on corrosion resistance and dross formation of Zn–23 wt % Al–0.3 wt % Si–x wt % Mg alloy. *Coatings*, *9*(3), 199. https://doi.org/10.3390/coatings9030199

[5] Masumoto, H. & Takebayashi, H. (1999). Bottom dross build-up in Al-Zinc coating bath. *PacZAC 99*, Kualalumpur, Malaysia.
[6] Luo, Q., Jin, F., Li, Q., Zhang, J. Y., & Chou, K. C. (2013). The mechanism of dross formation during hot-dip Al-Zn alloy coating process. *Journal for Manufacturing Science & Production*, *13*(1-2): 85-89. https://doi.org/10.1515/jmsp-2012-0023
[7] Khaliq, A., Parker, D. J., Setargew, N., Kondoh, K., & Qian, M. (2021). Dissolution kinetics of iron-based intermetallic compounds (τ 5c IMCs) in a commercial steel strip metallic alloy coating process. *Metallurgical and Materials Transactions B*, *52*(1), 41-50. https://doi.org/10.1007/s11663-020-01985-8
[8] Wu, G., Zhang, J., Li, Q., Chou, K., & Wu, X. (2011) Microstructure and Thickness of 55 pct Al-Zn-1.6 pct Si-0.2 pct RE Hot-Dip Coatings: Experiment, Thermodynamic, and First-Principles Study. *Metallurgical and Materials Transactions B*, *43*(1), 198-205. https://doi.org/10.1007/s11663-011-9578-2
[9] Shibli, S. M. A., Meena, B. N., & Remya, R. (2015). A review on recent approaches in the field of hot dip zinc galvanizing process. *Surface and Coatings Technology*, *262,* 210-215. https://doi.org/10.1016/j.surfcoat.2014.12.054
[10] Khaliq, A., Parker, D. J., Setargew, N., & Qian, M. (2020). Fabrication of the τ 5c intermetallic compound monoliths by a novel powder metallurgy and hot-dipping approach. *Metallurgical and Materials Transactions B*, *51*(2), 836-849 https://doi.org/10.1007/s11663-019-01765-z
[11] Chen, Z. W., Gregory, J. T., & Sharp, R. M. (1992) Intermetallic Phases Formed during Hot Dipping of Low Carbon Steel in a Zn-5 Pct AI Melt at 450 ºC. *Metallurgical and Materials Transactions A*, *23A*, 2393-2400. https://doi.org/10.1007/BF02658042
[12] Chen, R. Y. & Yuen, D. (2012). Microstructure and crystallography of Zn-55Al-1.6 Si coating spangle on steel. *Metallurgical and Materials Transactions A*, *43*(12), 4711-4723. https://doi.org/10.1007/s11661-012-1259-5
[13] Carpenter, K. R., Dippenaar, R., Phelan, D., & Wexler, D. (2007). Synthesis of intermetallics based on the Fe-Al-Si-zn alloy system by magneto-mechanical milling of ductile elemental powders. *Advanced Materials Research*, *15*, 1032-1037. https://doi.org/10.4028/www.scientific.net/AMR.15-17.1032
[14] Shawki, S. & Hamid Z. A. (2003), Effect of aluminium content on the coating structure and dross formation in the hot-dip galvanizing process. *Surface and Interface Analysis*, *35*(12), 943-947. https://doi.org/10.1002/sia.1608
[15] Phelan, D., Xu, B. J., & Dippenaar, R. (2006). Formation of intermetallic phases on 55wt.%Al–Zn–Si hot dip strip. *Materials Science and Engineering: A*., *420*(1-2), 144-149. https://doi.org/10.1016/j.msea.2006.01.085
[16] Mandal, G. K., Balasubramaniam, R., & Mehrotra, S. P., (2009). Theoretical Investigation of the Interfacial Reactions during Hot-Dip Galvanizing of Steel. *Metallurgical and Materials Transactions A*., *40*(3), 637-645. https://doi.org/10.1007/s11661-008-9748-2
[17] Giorgi, M. L., Guillot, J. B., & Nicolle, R. (2005). Theoretical model of the interfacial reactions between solid iron and liquid zinc-aluminium alloy. *Material Science*., *40*, 2263-2268. https://doi.org/10.1007/s10853-005-1944-5
[18] Luo, Q., Li, Q., Zhang, J. Y., & Lu, H. S. (2015) Microstructural evolution and oxidation behavior of hot-dip 55 wt.% Al–Zn–Si coated steels. *Journal of Alloys and Compounds*., *646*, 843-851. https://doi.org/10.1016/j.jallcom.2015.05.257
[19] Jordan, C. E. & Marder, A. R. (1997). Fe–Zn phase formation in interstitial-free steels hot-dip galvanized at 450ºC. *Material Science*., *32*, 5593-5602. https://doi.org/10.1023/A:1018680625668
[20] Khaliq, A., Chaudhry, I. A., Boujelbene, M., Ahmad, A., & Elbadawi, I. (2021). Iron-based intermetallic particles formation in Al-Zn-Si alloy through powder metallurgy route. *International journal of advanced and applied sciences*, *8*(12), 36-42. https://doi.org/10.21833/ijaas.2021.12.005
[21] Khaliq, A., Alghamdi, A. S., Ramadan, M., Subhani, T., Rajhi, W., Haider, W., & Hasan, M. M. (2022). Intermetallic Compounds Formation during 316L Stainless Steel Reaction with Al-Zn-Si Coating Alloy. *Crystals*, *12*(5), 735. https://doi.org/10.3390/cryst12050735
[22] Garcıa, F., Salinas, A., Nava, E., Mani, A., & Garza, R. (2004). Characterization of Dross Particles in an Industrial Galvalume Coating Bath. *Galvatech*, 1-8.

Contact information:

Abdul KHALIQ, Assistant Professor
(Corresponding author)
University of Ha'il
College of Engineering, University of Ha'il, Ha'il P.O. Box 2440, Saudi Arabia
E-mail: ab.ismail@uoh.edu.sa

Vishnu KASVA, Engineer
RMIT University,
College of Engineering, RMIT University, Melbourne, Australia
E-mail:vishnukasva@gmail.com

Abdulaziz S. ALGHAMDI, Professor
University of Ha'il
College of Engineering, University of Ha'il, Ha'il P.O. Box 2440, Saudi Arabia
E-mail: a.alghamdi@uoh.edu.sa

Mohamed RAMADAN, Professor
University of Ha'il
College of Engineering, University of Ha'il, Ha'il P.O. Box 2440, Saudi Arabia
E-mail: mrnais3@yahoo.com

Tayyab SUBHANI, Associate Professor
University of Ha'il
College of Engineering, University of Ha'il, Ha'il P.O. Box 2440, Saudi Arabia
E-mail: Tu.subhani@uoh.edu.sa

Waseem HAIDER, Professor
Central Michigan University,
School of Engineering and Technology, Central Michigan University, Mount Pleasant, MI 48859, USA
E-mail: haide1w@cmich.edu

K. S. Abdel HALIM, Professor
University of Ha'il
College of Engineering, University of Ha'il, Ha'il P.O. Box 2440, Saudi Arabia
E-mail: k.abdulhalem@uoh.edu.sa